

Subwavelength THz imaging of graphene photoconductivity

Samuel M. Hornett,* Rayko I. Stantchev, Martha Z. Vardaki, Chris Beckerleg,
and Euan Hendry

Physics Building, Stocker Road, University of Exeter, Exeter, Devon, UK, EX4 4QL

E-mail: s.m.hornett@exeter.ex.ac.uk

Contents

1	Spectrum of the THz Pulse	2
2	Optical Image of the Sample	3
3	Hadamard Image Formation	4
4	Phase Front Correction	6
	References	7

1 Spectrum of the THz Pulse

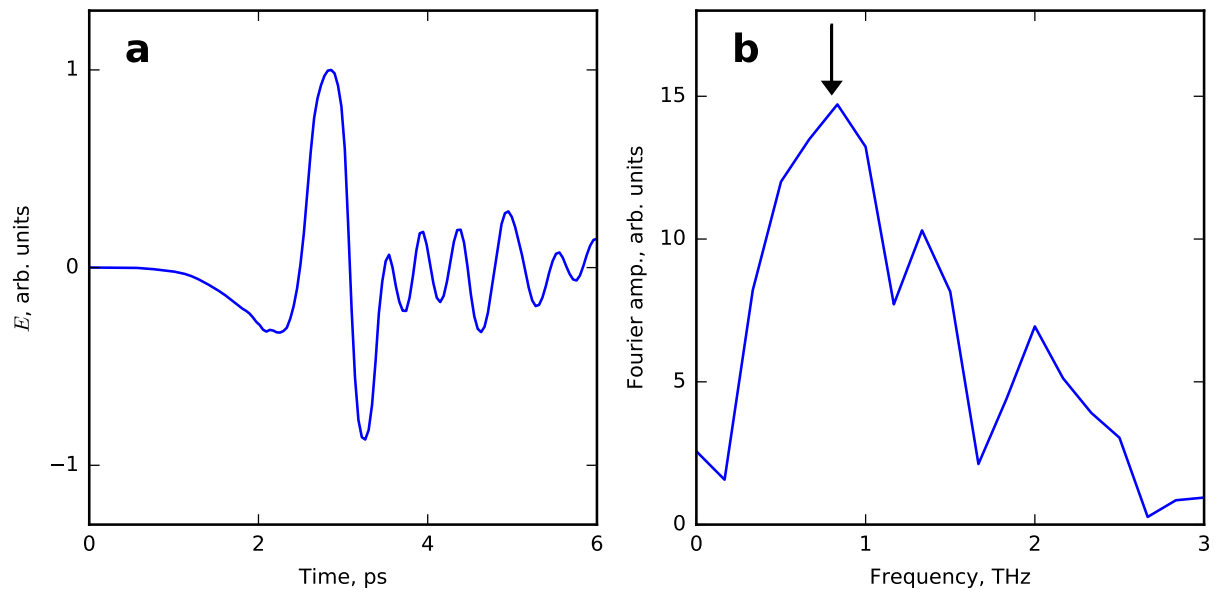


Figure 1: a. The electric field of our THz pulse recorded in the time domain using electro optic sampling as described in the main text. The oscillations after the pulse are due to the presence of water in the air. b. Fourier transform amplitude of our THz pulse with a peak at ≈ 0.8 THz (marked by arrow), again the dips in amplitude are due to water absorption resonances.

2 Optical Image of the Sample



Figure 2: White light reflection image of the sample area taken with a x20 objective on the Renishaw inVia system. This shows the graphene tare in the lower right corner, also observed in our Raman and THz images. Note that the field of view in the reflection measurements is rather small, and the repeating pattern seen is an artifact caused by stitching of separate images. This effect has been minimized by overlapping individual images and applying a background subtraction tool (WIRE software).

3 Hadamard Image Formation

Since we use single-element detector (our electro optic detection crystal), measurements for our images are obtained sequentially rather than in parallel. In such single-pixel imaging schemes optimal signal is achieved via the use of an orthogonal set of binary masking patterns derived from Hadamard matrices,^{1,2} which minimizes the mean square intensity noise in each pixel.¹ In our experimental setup, we can either photoexcite the graphene or not, implying that our masks have values either of 1s or 0s to denote which pixels have been sampled in each measurement. However, orthogonal Hadamard matrices are composed of +1s and -1s. In order to achieve this orthogonality in our measurement matrices, as is outlined in,² one carries out sequential measurements of a mask immediately followed by its inverse and the record difference in THz field transmission via a lock-in amplifier. This photo-induced difference in THz field transmission, ΔE , is related to the photoconductivity through equation 2 in the main text.

Using such a measurement, we can easily reconstruct a photoconductivity image. The construction of an N -pixel image Ψ is performed as follows: our i^{th} measurement, ϕ_i , is the dot product of the spatial transmission function of our object and the i^{th} mask configuration, mathematically expressed as

$$\phi_i = \sum_{j=1}^N w_{ij}\psi_j, \quad (1)$$

where w_{ij} is the spatial configuration of the i^{th} mask and ψ_j is the j^{th} image pixel. A convenient representation uses the matrix equation $\Phi = W\Psi$, where the rows of W are reformatted into the projected 2D masks. If the matrix W is invertible, the image vector Ψ is obtained via matrix inversion $\Psi = W^{-1}\Phi$. The final image is obtained by reshaping Ψ into a 2D array. Further, as stated earlier, our masks are derived from Hadamard matrices, i.e. W is a Hadamard matrix of order N . A Hadamard matrix H_n is defined as an $n \times n$ matrix of +1s and -1s with the property that the scalar product between any two distinct

rows is 0 (each row is orthogonal to every other one). Thus H_n satisfies:

$$H_n H_n^T = H_n^T H_n = nI_n, \quad (2)$$

where H_n^T is the transpose of H_n . This property means that the Hadamard inverse is $H_n^{-1} = H_n^T/n$, leading to a straightforward image reconstruction. In order to convert our spatial images of ΔE into photoconductivity, $\Delta\sigma$, we apply equation (2) in our paper.

4 Phase Front Correction

Figure 3 clarifies the experimental arrangement mentioned in the main text, whereby the phase front distortion added by the DMD is used in order to allow off axis photo-excitation without a corresponding time delay.

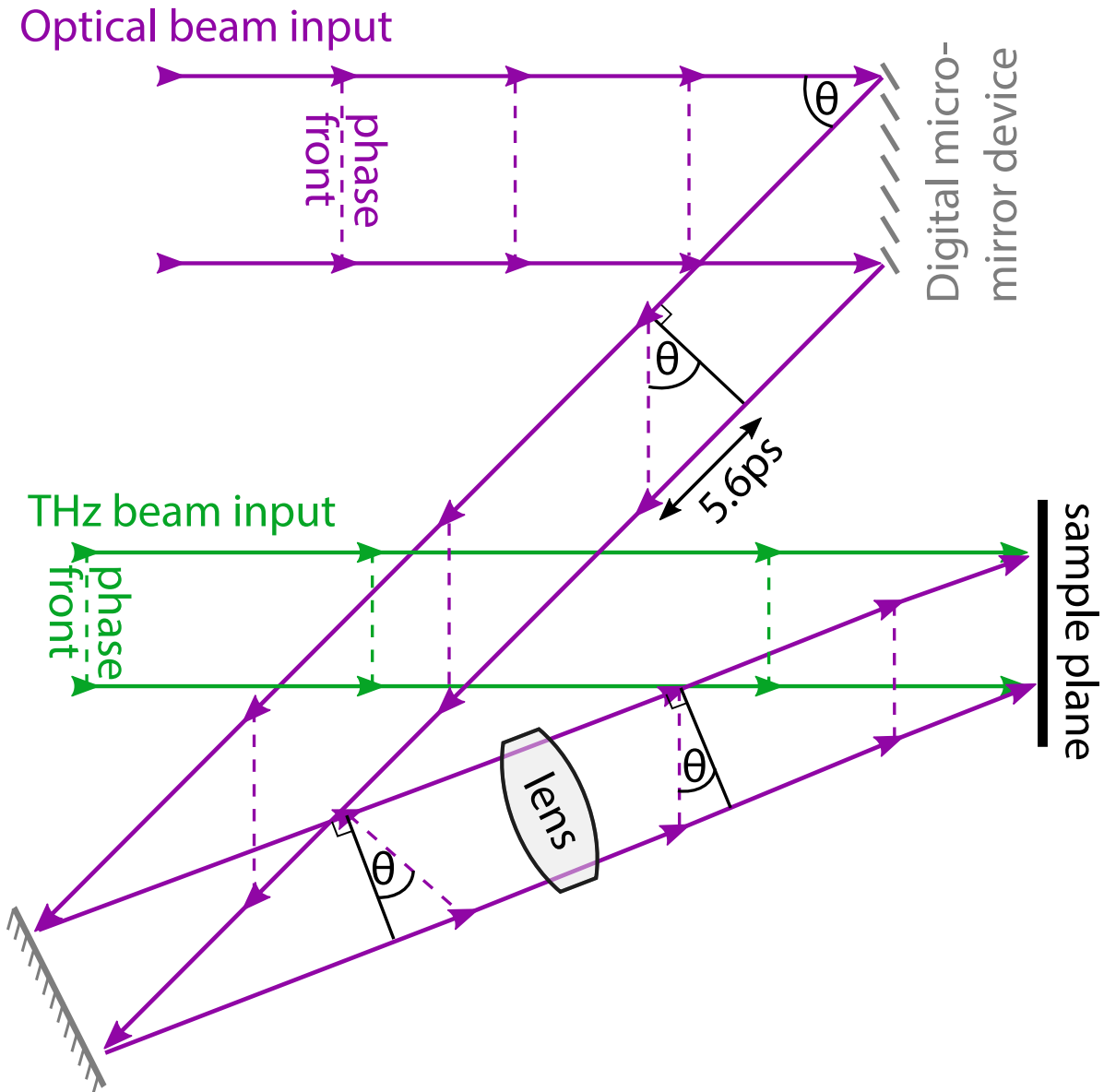


Figure 3: Diagram of the optical excitation scheme showing how a flat phase front is achieved with off axis photoexcitation. By using the phase front distortion introduced by the DMD mirror angle $\theta = 13^\circ$ to correct for the off axis excitation.

References

- (1) M. Harwit, and N. J. A. Sloane, (1979) *Hadamard Transform Optics* (Academic Press, New York, USA)
- (2) N. J. Sloane, Multiplexing Methods in Spectroscopy. *Mathematics Magazine*, 52 (1979), pp. 71–80